Received September 1999
Revised July 2000
Accepted July 2000

Entropy generation due to laminar forced convection flow past a parabolic cylinder

O.M. Haddad, M. Abu-Qudais and B.A/K Abu-Hijleh
Department of Mechanical Engineering, Jordan University of Science and Technology, Irbid, Jordan, and
A.M. Maqableh
Al-Balqa Applied University, Al-Huson Polytechnic, Al-Huson, Jordan

Keywords *Entropy, Forced convection, Flow, Cylinders*

Abstract *This study is focused on the local entropy generation of steady two-dimensional symmetric flow past a parabolic cylinder in a uniform stream parallel to its axis. The effect of both Reynolds number (Re) and temperature difference between the cylinder wall and the freestream (ΔT) on thermal, viscous, and total entropy generation is investigated for different values of Prandtl number (Pr) and Mach number (Ma). It was found that the thermal entropy generation increased as the temperature difference increased, while the viscous entropy generation decreased as Reynolds number increased. The results also showed that increasing Prandtl number or Mach number increased both the viscous and thermal contributions to the entropy generation.*

Nomenclature

a = nose radius of curvature
Ec = Eckert number, $U_\infty{}^2/(C_p\ \Delta T)$
f = modified stream function, (ψ/ξ)
g = modified vorticity
h = modified temperature, $-(\xi^2 + \mu^2)\theta/\xi$
k = thermal conductivity of fluid
Ma = Mach number, $(U_\infty/\sqrt{\lambda R T_\infty})$
Pr = Prandtl number, (v/α)
R = the gas constant
Re = Reynolds number based on the nose radius of curvature, (aU_∞/v)
S = overall entropy generation
S‴ = local entropy generation
T_w = wall temperature
T_∞ = free stream temperature
U_∞ = free-stream velocity
(x, y) = the Cartesian coordinates

Greek symbols
α = thermal diffusivity
γ = specific heat ratio
ΔT = the temperature difference, $(T_w - T_\infty)$
θ = non-dimensional temperature
μ = dynamic viscosity
ν = kinematic viscosity
(ξ, η) = the parabolic coordinates
Φ = viscous dissipation
ψ = stream function
ω = vorticity

1. Introduction

Every heat transfer process is accompanied by irreversibilities or entropy generation as a result of velocity and/or temperature gradients. In general, these irreversibilities cause a drop in the output power if the process is part of a power cycle and an increase in the input power if the process is part of a refrigeration cycle (Bejan, 1979). Thus our ability to reduce entropy generation or minimize the destruction of energy is related to the best efficient energy system design.

International Journal of Numerical Methods for Heat & Fluid Flow, Vol. 10 No. 7, 2000, pp. 770-779.

Local entropy generation in several simple flow situations with analytical solutions available for velocity and temperature fields has been evaluated by Bejan (1979, 1982). Theoretically, as long as the velocity and temperature gradients are known, entropy generation at each point in the flow field can be calculated. However, in case the geometric configuration is too complicated to perform theoretical approach, a numerical approach may be useful.

The minimization of entropy generation in ducts with heat transfer attracted considerable interest from engineers working on heat transfer augmentation techniques. Another large and diverse group of heat transfer devices relies on external convection, that is, heat transfer between a stream and a body immersed in the stream.

Flow past a parabola is of practical interest in aerospace. Aerodynamic bodies designed for subsonic flow generally have finite thickness distribution with a parabolic leading edge. Also, in turbomachinery applications, the cross-section of blades is usually similar to that of an airfoil.

The purpose of this study is to evaluate the local and global entropy generation of the laminar flow over a parabolic cylinder in uniform stream. The effect of the flow parameters on entropy generation will also be investigated. For this purpose, the velocity and temperature distributions of the laminar forced convection flow over a parabolic cylinder will be needed. In a previous work (Haddad *et al.*, 2000), the full Navier-Stokes and energy equations in stream function-vorticity variables were solved using the finite difference technique. The velocity and temperature profiles obtained by the previous study (Haddad *et al.*, 2000) are used in this study in order to calculate the entropy generated by the flow over the parabolic surface. To the best of the authors' knowledge, entropy generation due to convective heat transfer has been studied by many researchers, but none addressed the configuration presented herein.

2. Analysis

Figure 1 is a schematic diagram of the flow problem under consideration. The surface of the parabola is defined by the following equation:

$$x(y) = \frac{1}{2a}\left(y^2 - a^2\right)$$

where the constant (a) is recognized as the nose radius of curvature. The steady state equations for laminar forced convection flow over a parabolic cylinder in Cartesian co-ordinates can be written in the following form (Haddad and Corke, 1998):

$$\psi^*_{xx} + \psi^*_{yy} = -\omega^* \tag{1}$$

$$\psi^*_y \omega^*_x - \psi^*_x \omega^*_y = \upsilon\left(\omega^*_{xx} + \omega^*_{yy}\right) \tag{2}$$

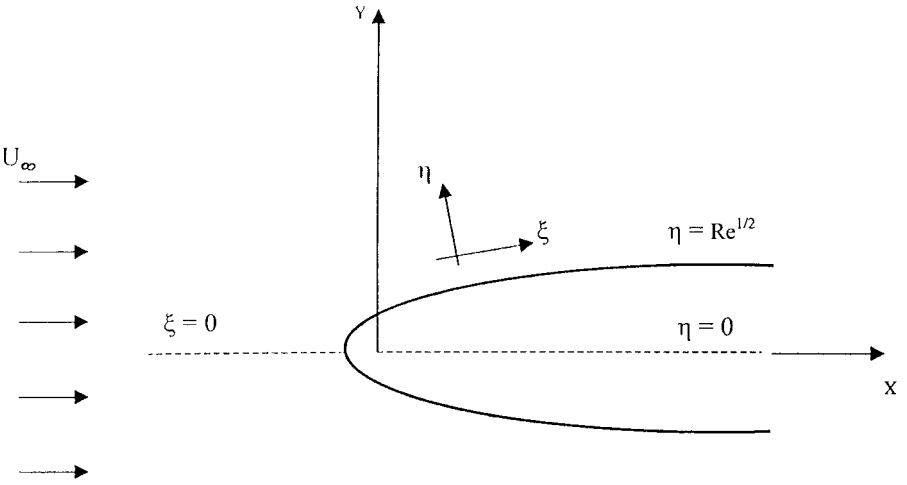

Figure 1.
Schematic diagram of the flow problem

$$\psi_y^* T_x^* - \psi_x^* T_y^* = \alpha\left(T_{xx}^* + T_{yy}^*\right) \tag{3}$$

where ψ and ω are the stream function and vorticity, respectively, and the star indicates a dimensional quantity. Equation (3) is added to equations (1) and (2) listed in the reference mentioned above in order to obtain the solution of the thermal part of the problem.

These equations are subjected to the following boundary conditions:

- At the wall ($y = y_w$): we consider the no-slip, no-penetration conditions on an isothermal wall

$$\psi^* = \text{constant} = 0,\ \frac{\partial \psi^*}{\partial y*} = 0,\ \omega^* = -\psi_{yy}^* \text{ and } T^* = T_w^*$$

- At the freestream: we consider uniform (potential) flow of an isothermal fluid

$$\psi^* = \psi_\infty,\ \omega^* = 0 \text{ and } T^* = T_\infty^*$$

The local entropy generation can be calculated from the following equation (Bejan, 1982):

$$\begin{aligned} S'''^*(x,y) &= \frac{k}{T^{*2}}(\nabla T)^2 + \frac{\mu}{T^*}\Phi \\ &= \text{thermal component} + \text{viscous component} \\ &= \frac{k}{T^{*2}}\left[\left(\frac{\partial T^*}{\partial x^*}\right)^2 + \left(\frac{\partial T^*}{\partial y^*}\right)^2\right] + \frac{\mu}{T^*}\left\{4\left[\frac{\partial \psi^*}{\partial x^* \partial y^*}\right]^2 + \left[\frac{\partial^2 \psi^*}{\partial y^{*2}} - \frac{\partial^2 \psi^*}{\partial x^{*2}}\right]^2\right\} \end{aligned} \tag{4}$$

The first term on the right-hand side of equation (4) represents the entropy generation due to the thermal effect (temperature gradients) while the second term represents the entropy generation due to viscous effect (velocity gradients).

Introducing the following non-dimensional groups:

$$x = \frac{x^*}{(\upsilon / U_\infty)}, y = \frac{y^*}{(\upsilon / U_\infty)}, \omega = \frac{\omega^*}{\left(U_\infty^2/\upsilon\right)},$$

$$\psi = \frac{\psi^*}{\upsilon}, \theta = \frac{T^* - T_\infty^*}{T_w^* - T_\infty^*}, S = \frac{S^*}{k(U_\infty/\upsilon)^2}$$

$$\text{and } \sigma = \frac{\mu U_\infty^2}{k\left(T_w^* - T_\infty^*\right)} = \Pr Ec$$

and to convert the equations from the cartesian coordinate system (x, y) to the parabolic coordinate system (ξ, η), we use the following relation:

$$(\mathrm{x} + \mathrm{iy}) = \frac{(\xi + \mathrm{i}\eta)^2}{2}$$

where i here is $\sqrt{-1}$. The resulting equations are then expressed in terms of the new functions f, g, and h variables, using the following definitions:

$$\psi = \xi f(\xi, \eta), \quad \omega = -\frac{\xi}{(\xi^2 + \eta^2)} g(\xi, \eta) \quad \theta = -\frac{\xi}{(\xi^2 + \eta^2)} h(\xi, \eta)$$

The purpose of this transformation is to obtain stream-function and vorticity equations similar to those obtained by Davis (1972). The final form of the governing equations (1)-(3) becomes as follows:

$$\mathrm{f}_{\eta\eta} - \mathrm{g} + \left(\mathrm{f}_{\xi\xi} + \frac{2}{\xi}\mathrm{f}_\xi\right) = 0 \tag{5}$$

$$\begin{aligned} \mathrm{g}_{\eta\eta} + \left(\mathrm{f} + \xi\mathrm{f}_\xi - \frac{4\eta}{\xi^2 + \eta^2}\right)\mathrm{g}_\eta + \left(\frac{\xi^2 - \eta^2}{\xi^2 + \eta^2}\mathrm{f}_\eta - \frac{2\eta}{\xi^2 + \eta^2}(\mathrm{f} + \xi\mathrm{f}_\xi)\right)\mathrm{g} \\ -\xi\,\mathrm{g}_\xi\left(\mathrm{f}_\eta + \frac{4}{\xi^2 + \eta^2}\right) + \left(\mathrm{g}_{\xi\xi} + \frac{2}{\xi}\,\mathrm{g}_\xi\right) = 0 \end{aligned} \tag{6}$$

$$\begin{aligned} \mathrm{h}_{\eta\eta} + \left(\Pr(\mathrm{f} + \xi\mathrm{f}_\xi) - \frac{4\eta}{\xi^2 + \eta^2}\right)\mathrm{h}_\eta + \Pr\left(\frac{\xi^2 - \eta^2}{\xi^2 + \eta^2}\mathrm{f}_\eta - \frac{2\eta}{\xi^2 + \eta^2}(\mathrm{f} + \xi\mathrm{f}_\xi)\right) \\ \mathrm{h} - \xi\mathrm{h}_\xi\left(\Pr\mathrm{f}_\eta + \frac{4\xi}{\xi^2 + \eta^2}\right) + \left(\mathrm{h}_{\xi\xi} + \frac{2}{\xi}\mathrm{h}_\xi\right) = 0 \end{aligned} \tag{7}$$

and the boundary conditions take the following final form:

- at the wall ($\eta = \mathrm{Re}^{1/2}$):

$$f = 0,\ \frac{\partial f}{\partial \eta} = 0,\ \mathrm{g}|_{\mathrm{wall}} = \mathrm{f}_{\eta\eta} \text{ and } h|_{\mathrm{wall}} = -\frac{\xi^2 + \mathrm{Re}}{\xi}$$

- at the free stream ($\eta \to \infty$):

$$\frac{\partial f}{\partial \eta}|_{\eta\to\infty} \to 1,\ g|_{\eta\to\infty} \to 0 \text{ and } h|_{\eta\to\infty} \to 0$$

The final form of the local entropy generation rate (equation (4)) in parabolic coordinates becomes:

$$\begin{aligned} S'''(\xi,\eta) = {} & \frac{1}{(\theta+\bar{\theta})^2}\left[\left(\theta_\eta^2 + \theta_\xi^2\right)\left(\eta_x^2 + \eta_y^2\right)\right] \\ & + \frac{\sigma}{(\theta+\bar{\theta})}\left[4\left(\psi_\eta^2 + \psi_\xi^2\right)\left(\eta_{xx}^2 + \xi_{xx}^2\right) + \left(\psi_{\eta\eta} - \psi_{\xi\xi}\right)\right. \\ & \left.\left[\left(\eta_y^2 - \eta_x^2\right)\left(1 - 4\left(\psi_\eta\eta_{xx} + \psi_\xi\xi_{xx}\right) + 8\eta_x\eta_y\left(\psi_\eta\xi_{xx} - \psi_\xi\eta_{xx}\right)\right)\right]\right] \end{aligned} \tag{8}$$

where, for convenience, $\bar{\theta} = \dfrac{T_\infty^*}{T_w^* - T_\infty^*}$.

The overall entropy generation can be calculated by integrating the local entropy equation over the entire domain using the following equation:

$$S_{tot} = \int_0^{\xi_{\max}} \int_{\eta_{wall}}^{\eta_{\max}} S'''(\xi,\eta)\, d\eta\, d\xi \tag{9}$$

3. Numerical solution

The non-dimensional form of the governing equations (5)-(7) with their boundary conditions were discretized using a second-order accurate finite difference scheme on a non-uniform grid. A uniform grid was first generated and then Robert's stretching transformation (Anderson *et al.*, 1984) was applied in both streamwise and wall normal direction in order to cluster more points near the leading edge in one direction and near the wall in the other direction. The governing equations were linearized using Newton's linearization technique. Three points central difference formulas were used whenever possible (interior points); otherwise backward or forward difference formulas were used as applicable (boundary points). The resulting system of linear algebraic equations was solved simultaneously by iteration using the proper LINPACK subroutines (Dongarra *et al.*, 1979) with the coefficient matrix being of the banded matrix type. All computations were performed in double

precision arithmetics. More details on the numerical method are given by Haddad *et al.* (2000). In general, the solution required seven iterations to converge to a maximum local error of 10^{-5}. The calculations were performed on a "digital" (alpha processor) Unix workstation.

It is worthy of mention here that it was necessary to reduce the number of boundary conditions at the wall from four to three. This was accomplished by discretizing the first two of these boundary conditions, then substituting one equation into the other; thereby the two boundary conditions were merged into one equation. In addition, one should note that the numerical plane must be finite in both streamwise and wall normal directions. It is well-known that for a parabolic cylinder the flow proceeds without separation from a stagnation point flow at the nose to a Blasius flow far downstream. Based on the study made by Haddad and Corke (1998), the freestream was located at a distance from the wall equivalent to ten times the downstream Blasius boundary layer thickness on a flat plate of the same length as the parabola. Also, in the streamwise direction, the outflow boundary was located at a distance from the leading edge far enough for the Blasius flow to be reached. This fact will be confirmed by the results.

Davis (1972) showed that excluding the elliptic terms (the last two terms) in each of the governing equations (5) and (6)) results in equations which contain both the first order boundary layer terms and the terms for the second order curvature correction. Based on this, the boundary conditions at the outflow are derived by applying the governing equations at the outflow with the elliptic terms being dropped out. This treatment has the advantage of not imposing any solution at downstream infinity (e.g. Blasius solution); nevertheless, we can still compare our solution with the flat plate Blasius solution to validate our approach. To implement this, a buffer zone was specified in which the elliptic terms in the governing equations were multiplied by a weighting factor, $S(i)$. The weighting factor was a function of the streamwise location only. At the beginning of the buffer zone, $S(i) = 1$, while at the end of the buffer zone which corresponds to the outflow boundary, $S(i) = 0$. In order to effect a smooth transition from $S(i) = 1$ to $S(i) = 0$, the weighting factor was given the following form

$$S(i) = \frac{1 + \tanh(\arg)}{2}$$

where

$$\arg = 4\left[1 - \frac{2(i - ibuf)}{(I_{\max} - ibuf)}\right]$$

where (i) is the numerical index in the streamwise direction and *ibuf* is the index (i) at the beginning of the buffer-zone. The governing equations were solved for the f, g and h variables. The results were then used to estimate both local and total entropy generation.

4. Results and discussion

Numerical test calculations were carried out to evaluate the effect of grid size (i.e. number of grid points) on the obtained solution. Attention was focused on the wall vorticity to judge the solution sensitivity. It was found that the numerical results were more sensitive to the total number of grid points in the wall normal direction (J_{max}) than in the streamwise direction (I_{max}). Almost identical results were obtained for the cases with I_{max} = 150 and I_{max} = 350, whereas significant changes in the solution occurred when J_{max} was changed from 30 to 33. The solution was invariant for $J_{max} > 33$; thus a grid size of 200 × 36 points was used throughout this study.

The main focus of this study was the changes in total entropy generation as a function of the main parameters that define the flow, i.e. Reynolds number (Re), Mach number (Ma), and temperature difference (ΔT). The effect of fluid type manifested in the fluid's Prandtl number was also studied. The relative contribution of the viscous and thermal components of entropy generation are shown and discussed.

Figure 2 shows the changes in the viscous and thermal entropy generation as a function of the Reynolds number (Re) for different fluids. The three fluids shown, which span the range of Prandtl numbers, showed similar trends. The only difference was the magnitude of entropy generation which increased with Prandtl number due to the higher viscosity of the fluid. Although Figure 2 is shown for a single combination of Mach number and temperature difference,

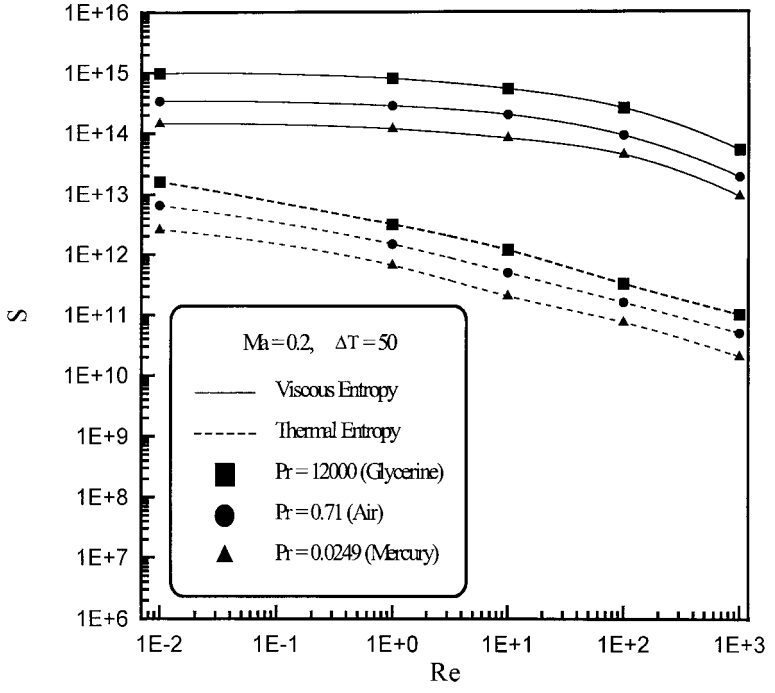

Figure 2.
The effect of Reynolds number (Re) on viscous and thermal entropy generation at differential Prandtl numbers (Pr)

the previous observation was true for several other calculated combinations of Ma and ΔT and is not reported herein for brevity. Thus, the remainder of this paper will focus on air but the conclusions should hold for any other fluid.

Figure 3 shows the changes in entropy generation as a function of Reynolds number for several values of Mach number. It is clear that the viscous contribution to entropy generation was dominant for all values of Reynolds number and all those of Mach number. Both viscous and thermal entropy generation decreased as the Reynolds number increased. Recall that Re is based on the nose radius of curvature. Thus, a higher Re means a parabola with a more rounded nose which translates to a more gradual change in fluid velocity as it flows over the nose. A reduction in the velocity gradients results in a reduction in the viscous entropy generation, as per the last term in equation (4). Also, the rounder nose results in smaller temperature gradients which lead to a reduction in the thermal entropy generation, as per the first term on the right hand side of equation (4). Figure 3 shows an interesting feature when comparing entropy generation at different Mach numbers. An increase in Mach number results in an increase in entropy generation. This is a logical result due to the increased difference between the free stream velocity and the zero velocity at the wall. The result is a higher velocity gradient and more entropy generation. The interesting note is that the biggest rise in entropy generation occurred at low Mach number, between 0 and 0.1. As the Mach number increased the extra rise in entropy generation was not as great as in the range 0 to 0.1. This has to deal with the non-linear growth rate of boundary layer

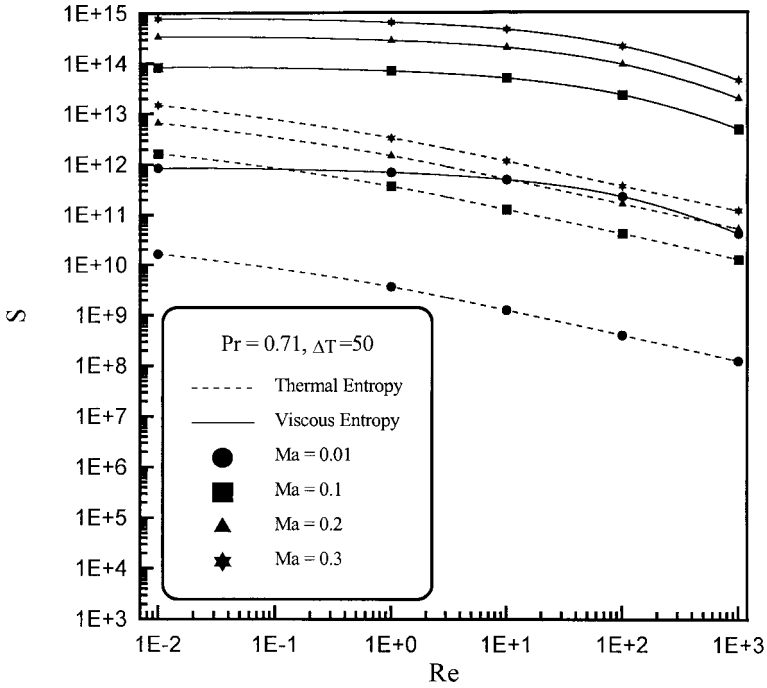

Figure 3.
The effect of Reynolds number (Re) on viscous and thermal entropy generation at differential Mach numbers (Ma)

thickness with increased Mach number. The highest Mach number shown in Figure 3 was 0.3, which means that the flow is still incompressible. This is important as the code used does not allow for variable fluid properties, especially density.

Figures 4 and 5 show the effect of temperature difference on entropy generation for different Mach and Reynolds numbers, respectively. As expected, changes in the temperature difference had no effect on the viscous entropy generation. The temperature difference affects only the thermal entropy generation in the form of higher temperature gradients in the transverse direction. The viscous entropy generation was the dominant term for all Mach and Reynolds numbers even at the largest value of ΔT. This result is important from a design point of view and suggests that any effort towards the reduction of total entropy should focus on reducing the viscous contribution. The secondary role of thermal effects on the total entropy generation supports our decision to neglect the viscous dissipation term in the energy equation (equation (3)).

5. Conclusions

The effects of Mach number, temperature difference, nose radius, and fluid type on the total entropy generation due to laminar incompressible flow over a parabola was studied numerically. The general trend of entropy generation was similar for all fluids studied. The entropy generation due to viscosity was the dominant form of entropy generation for all values of Mach number,

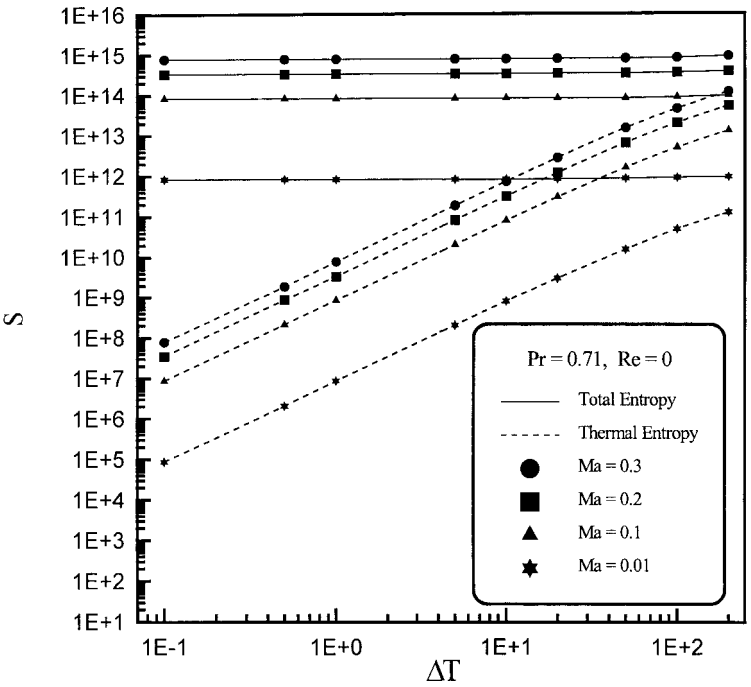

Figure 4.
The effect of temperature difference (ΔT) on entropy generation at different Mach numbers (Ma)

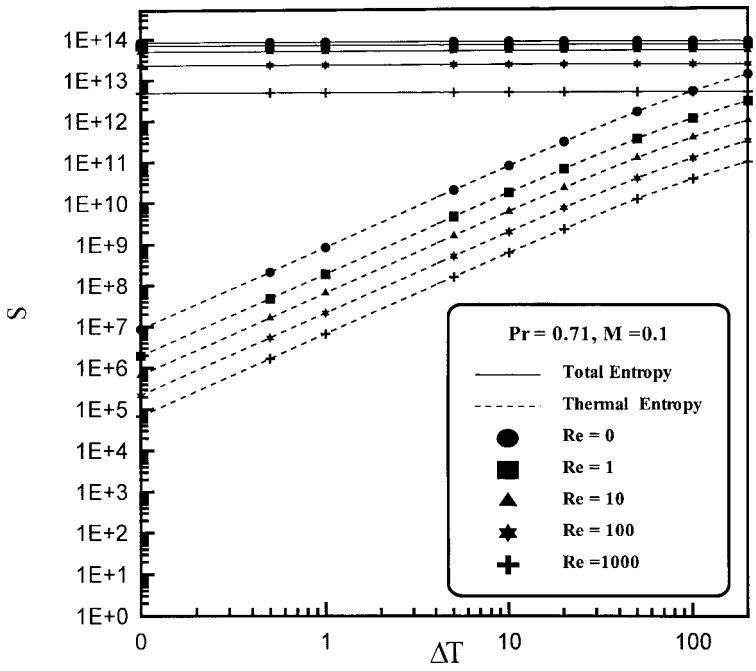

Figure 5.
The effect of temperature difference (ΔT) on entropy generation at different Reynolds numbers (Re)

Reynolds number, and temperature difference. The entropy contribution due to thermal effects played a secondary role. The results showed that changes in the entropy generation were not linear with respect to changes in the Mach number nor Reynolds number. Further work on reducing entropy generation should focus on controlling the hydrodynamics of the flow and not the temperature field.

References

Anderson, D.A., Tannehill, J.C. and Pletcher, R.H. (1984), *Computational Fluid Mechanics and Heat Transfer*, Hemisphere Publishing Corp.

Bejan, A. (1979), "A study of entropy generation in fundamental convective heat transfer", *ASME Journal of Heat Transfer*, Vol. 101, pp. 718-25.

Bejan, A. (1982), *Entropy Generation through Heat and Fluid Flow*, Wiley Interscience, New York, NY.

Davis, R.T. (1972), "Numerical solution of Navier-Stokes equations for symmetric laminar incompressible flow past a parabola", *Journal of Fluid Mechanics*, Vol. 51, pp. 417-33.

Dongarra, J.J., Moler, C.B., Bunch, J.R. and Stewart, G.W. (1979) , *LINPACK Users' Guide*, Siam.

Haddad, O.M. and Corke, Th.C. (1998), "Boundary layer receptivity to free-stream sound on parabolic bodies", *Journal of Fluid Mechanics*, Vol. 368, pp. 1-26.

Haddad, O.M., Abu-Qudais, M. and Maqableh, A.M. (2000), "Numerical solution of the Navier-Stokes and energy equations for laminar incompressible flow past parabolic bodies", *International Journal of Numerical Methods for Heat and Fluid Flow*, Vol. 10 No. 1, pp. 80-93.